Challenging Glass 5 – Conference on Architectural and Structural Applications of Glass
Belis, Bos & Louter (Eds.), Ghent University, June 2016.

ISBN 978-90-825-2680-6

Fracture Simulation of Structural Glass by Element Deletion in Explicit FEM

J. Pelfrene, S. Van Dam, R. Sevenois, F. Gilabert & W. Van Paepegem
Ghent University, Department of Materials Science and Engineering, Belgium,
joren.pelfrene@ugent.be

In finite element simulation of glass cracking for practical engineering problems, the method of element deletion is often used despite its shortcomings. With this technique, an element is removed from the system upon reaching a certain failure criterion. Many different formulations for the failure behaviour of an element are possible, differentiated by the physical correctness of their representation and by their implications on the numerical stability of the calculation. In this paper, three failure models are characterised by use of a unit element model and evaluated for the drop weight impact on a monolithic glass plate. Several issues can be identified: (i) incorrect calculation of fracture energy for large-sized elements; (ii) shock wave propagation upon deletion of an element leading to spurious failure of other elements; (iii) unrealistic crack formation when the failure model does not account for crack directionality. A crack delay failure model for structural glass is proposed to avoid the aforementioned problems. This failure model uses only physical material properties as input and limits the damage rate during fracture.

Keywords: Glass, Brittle, Fracture, FEM, Element Deletion

1. Introduction

The accurate prediction of the fracture behaviour of glass and other brittle materials can be of great interest in a multitude of events. Possible cases include the assessment of the post-fractured load-bearing capacity of reinforced concrete or laminated glass components (Louter and Nielsen 2009), forces exerted by a breaking windshield on humans in a crash (Peng et al., 2013), arrest or penetration of a ballistic projectile (Brajer et al. 2010), window resistance to blast loading (Pelfrene et al., 2016), and many others.

The finite element method (FEM) provides a versatile tool to simulate both local and global forces and deformations, and can give information about the energy absorption in a dynamic event. Over the years, extensive advances have been made in the numerical simulation of crack initiation and propagation in solid materials. Several approaches have been developed in order to describe the evolution of a crack, e.g. cohesive zone elements (Camacho and Ortiz 1996), extended finite element method (XFEM) (Moës et al., 1999), meshless (Belytschko et al. 1995) and particle conversion methods (Johnson et al. 2002). Despite these efforts, still many challenges remain, especially for coupled problems and dynamic failure of thin-walled structures. The simulation of glass breakage in particular requires the modelling of crack branching and intersection in transient dynamics which cannot be treated by several advanced methods. Furthermore, windows are typically thin-walled with a large surface. When meshless methods or cohesive zone approaches are used, the analysis for such a structure requires an extremely high amount of elements which is detrimental for the computational efficiency. For correct representation of interlayer polymers in laminated glass by highly non-linear material models and interactions with the supporting structure an extensive, usually commercial, FE software package is preferred.

With all requirements, to date only the more crude approach to crack simulation by element deletion can practically be applied for the simulation of glass under low velocity impact or blast. This technique is relatively simple to implement and can be coupled with any failure criterion or damage. In engineering applications, the initiation of failure is commonly governed by a local strain or stress-based criterion. An often mentioned drawback is the removal of mass from the model, which conflicts with the conservation laws. However, most finite element codes do not actually delete the mass, but reduce the material stiffness of the element to zero. More grave are the very high degree of mesh dependency and occasional instabilities reported for this method (Song et al. 2006). From the fracture mechanics point of view, element deletion is insensitive to the size effect of strength and the element meshes used in engineering applications are commonly too coarse to capture gradients near the crack tip which leads to an overestimation of the fracture energy (Unosson et al. 2006). Fracture models with element deletion should therefore be used and interpreted with caution.

In this paper, crack simulation by element deletion is evaluated for correctness, stability and accuracy. First, a description of the physical nature of glass fracture is given. In Section 3, the characteristics of three different failure models are examined using a simple model with a single, failing unit element. The third failure model is introduced

as a new failure model for element deletion and has been specifically designed with glass in mind. This implementation attempts to overcome some of the issues experienced with the others. The failure models are further compared for the case of a monolithic glass specimen in a drop weight impact experiment in Section 4.

2. Brittle fracture of glass

The technical strength of glass is of great importance in the dimensioning of a structure and, in this paper, to realistically capture the cracking and fragmentation of a glass specimen. It is well known that the glass strength is not a unique value. Because glass is not capable of plastic deformation on a macroscopic scale, it is highly sensitive to surface flaws and inhomogeneities in its microstructure. Once the loading reaches the point where one critical flaw can extend, it grows quickly into a visible crack completely splitting the sample. The macroscopic strength is thereby dependent on the size, shape and orientation of the flaws in the material. A size effect exists, as it is probable that a large glass panel contains a weaker critical flaw than a smaller specimen. The Weibull distribution is an appropriate mathematical expression of the weakest link principle and has in the past been reported to provide the best statistical representation of the strength of glass specimens (Behr et al. 1991). In general, the most critical flaws are found on the cut and machined glass edges. The effect of edge flaws on the strength of a glass panel is described in the work of Veer et al. (2011), who also discuss corrections to the standard Weibull theory.

Criteria for the crack extension of a single flaw in an elastic-brittle material are described in the field of linear elastic fracture mechanics (LEFM). In general, for brittle materials only cracking in Mode I, the tensile opening mode, needs to be considered. The asymptotic stresses around the crack tip are then defined in function of the stress intensity factor K_I, first introduced by Irwin (1957). A crack may grow when the stress intensity factor reaches a critical value, i.e. the fracture toughness K_{Ic}. The fracture toughness of soda-lime silicate glass has been determined experimentally by different authors. A recent paper by Surdyka et al. (2014) gives the following values: K_{Ic} = 0.77 MPa m$^{1/2}$ in water, and 0.81 MPa m$^{1/2}$ in air with 40% relative humidity. Under the influence of the surrounding environments, flaws may also increase in size at a stable, low velocity. This is termed subcritical crack growth and is the mechanism behind the reduction of the technical glass strength over time. Beason and Morgan (1984) described the effect of load duration on the glass strength in ambient air, for which the simplified formulation is given in Eq. 1.

$$\sigma_{60} = \sigma_{t_d}\left(\frac{t_d}{60}\right)^{1/16} \tag{1}$$

where t_d is the load duration and σ_{60} is the fracture strength corresponding with a load imposed for 60 s.

A fracture criterion can also be formulated by considering the energy balance of the system. Griffith (1920) recognised that extension of a crack requires an amount of energy to be expended at a microscopic level to create new free, cracked surface. This fracture energy G_c is the critical value for the energy release rate. For the pure Mode I case, a unique relation exists between the energy release rate and the stress intensity factor, which also holds for their critical values (Irwin, 1957):

$$G_I = \frac{K_I^2}{E} \qquad \text{for plane stress} \tag{2}$$

$$G_I = (1-\nu^2)\frac{K_I^2}{E} \qquad \text{for plane strain} \tag{3}$$

Assuming K_{Ic} = 0.77 MPa m$^{1/2}$ and plane strain conditions, this yields G_{Ic} = 8.66 J/m^2 for a stationary crack. The fracture energy for soda lime silicate glass has also been determined experimentally by various methods. The experimentally obtained values for a selection of papers are given in Table 1.

Table 1: Fracture energy of soda lime silicate glass in ambient air.

Author(s)	Method	Fracture energy [J/m^2]
Clif (1957)	Cone crack test	7.4 – 8.6
Linger and Holloway (1968)	Double cantilever cleavage	6.6 – 7.8
Wiederhorn (1969)	Double cantilever cleavage	7.82
Sharon and Fineberg (1999)	Notched sheet tensile test	30 – 40

It is notable that the fracture energy measured by Sharon and Fineberg (1999) is much higher than the other values in Table 1. They account for the fracture energy measured on a dynamically propagating crack. The crack propagation velocity is in theory only bounded by the Rayleigh wave speed (c_R = 3310 m/s for soda lime glass). In practice, a certain stability limit exists at which micro-crack branches appear which slow down the crack propagation and arrest as the energy directed into each branch decreases. As this process repeats, the main crack moves at a nearly constant speed, which, for soda lime glass, is v_c = 1500 m/s. Sharon and Fineberg (1999) concluded that the apparent increase in fracture energy at high crack velocity is simply explained as the energy required to create new fracture surface for both the main crack and its micro-scale branches.

While the glass strength decreases with age, an apparent increase of the strength is noted when a high loading rate is applied. According to Gehrke et al. (1987), the influence of the surrounding medium on the material strength cannot entirely be excluded for loading rates up to 10^6 MPa/s. This is confirmed by Nie et al. (2010), who used the split-Hopkinson pressure bar to perform dynamic ring-on-ring tests on circular samples of borosilicate glass with different surface roughness. Moreover, the specimens with ground and polished edges show the same trend for relative strength increase with loading rate. An interpolated function, based on the data by Nie et al., is given in Fig. 1. This function enables calculation of the strength increase under dynamic loading if it can be assumed that soda lime silicate glass follows the same trend as borosilicate glass.

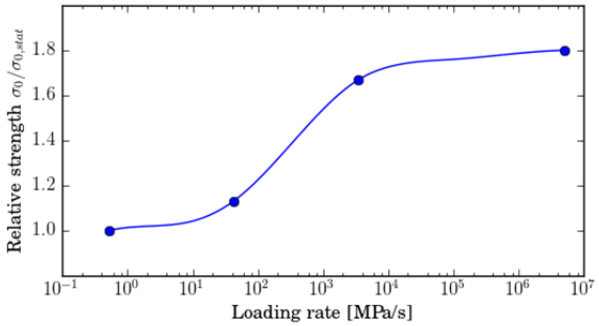

Fig. 1 Strength increase with loading rate for borosilicate glass (after Nie et al. (2010)).

3. Numerical implementation of failure models for element deletion

3.1. Immediate element failure

A very straightforward approach to crack simulation by element deletion consists of immediately removing the element upon reaching a failure criterion. This approach has been used by many authors, not only for the simulation of glass fracture, but for a great variety of problems. In essence, the stiffness matrix of an element is set to zero within one time increment of reaching a failure criterion at one or more of its integration points. No damage softening phase is included, nor is the directionality of the crack taken into account.

Such failure model is not readily available in the commercial FE software ABAQUS, but can easily be implemented for a linear elastic-brittle material as a user-defined material model for explicit analysis. The Rankine principal stress criterion is used as fracture criterion for brittle material on the macroscale. The behaviour of this material model is evaluated by use of a simple model consisting of a unit element, as shown in Fig. 2a. The elastic-brittle material for this example is given material properties with rounded values, listed in Table 2.

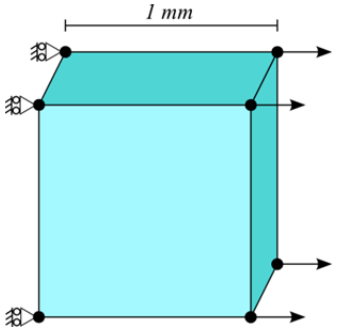

Fig. 2 Unit element model.

Table 2: Material properties for unit element example.

Young's modulus	E	100 GPa
Poisson's ratio	ν	0.25
Fracture strength	σ_0	100 MPa
Density	ρ	$2.5 \cdot 10^9$ kg/m^3

To avoid dynamic effects in the elastic phase, the inertia is increased by setting an artificially high density. This also results in a higher stable time increment in accordance with the CFL condition. The left side nodes of the element are held fixed in horizontal direction while on the right side nodes a horizontal displacement of 4 µm is imposed over the duration of 1 s. The fracture strength should be reached when the strain amounts to 0.1% in uniaxial tension, which occurs when the displacement of the right nodes is u_0 = 1 µm. Fig. 3 shows the stress evolution and the energies in the model in function of the displacement. When the failure stress is reached, the element can no longer bear any load. All strain energy within the element at that moment is dissipated at once as the material stiffness becomes zero. Subsequently, no stress oscillations occur and no energy is viscously dissipated by damping of stress waves.

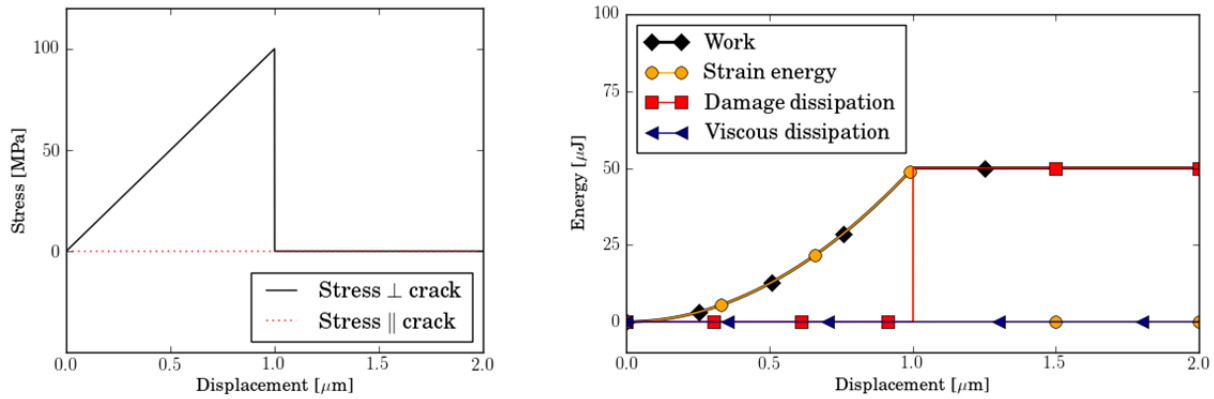

a) b)

Fig. 3a) Stress components and b) Energies in function of displacement for unit element model with immediate failure.

The situation would be different for surrounding elements that do not fail. Therefore, a model with three unit elements in a row is considered for which only the middle element can fail. The free nodes of the leftmost element are held fixed and those of the rightmost element are given a displacement of 12 µm in 1 s. The energies for such model are given in Fig. 4. It is seen that one third of the strain energy upon fracture is dissipated as damage, which corresponds with the failure of the middle element. The outer two elements are suddenly released and show heavy oscillations which are damped by the bulk viscosity. In the article by Song et al. (2006), it is the reflection and interference of these stress waves that causes unexpected failure of elements away from the crack tip in a larger simulation. This is presumably also the cause of instabilities experienced in the simulation of the blast response of a laminated glass panel using this failure model in LS-DYNA (Pelfrene et al. 2016).

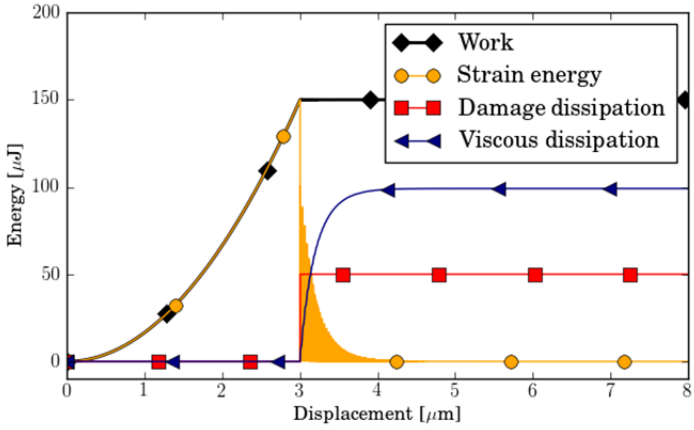

Fig. 4 Evolution of energies in function of displacement for unit element model with immediate failure.

3.2. Hillerborg model

Hillerborg et al. (1976) introduced a smeared crack model for concrete in finite elements by use of the cohesive zone concept. The smeared formulation denotes that a macro-crack is not represented explicitly, but rather that the model takes account of the effect of cracking in the form of an elastic stiffness reduction at the integration points of an element. Fig. 5 schematically shows the behaviour of this model in the way that it is implemented as a built-in material model (*Brittle Cracking) for ABAQUS/Explicit. The Rankine fracture criterion is used, i.e. a crack initiates when the maximum principal stress reaches the material strength σ_0. Once a crack has initiated, the tensile stress perpendicular to the crack decreases with increasing crack width until the work performed on the element matches the fracture energy G_{Ic}. At that point, the element can no longer bear any tension in that direction. Compression can still be supported when the crack closes. The tensile softening is then halted until the crack grows again. During the damage phase, also the shear stiffness $G_{||}$ for shearing in the crack plane is reduced and becomes zero at a crack opening displacement u_{cs}. Additionally, a crack opening displacement u_{cu} at ultimate failure of the element may be defined, at which point the element is deleted from the simulation. Before u_{cu} is reached, additional cracks may initiate at the element's integration points, but only in a direction perpendicular to the original crack.

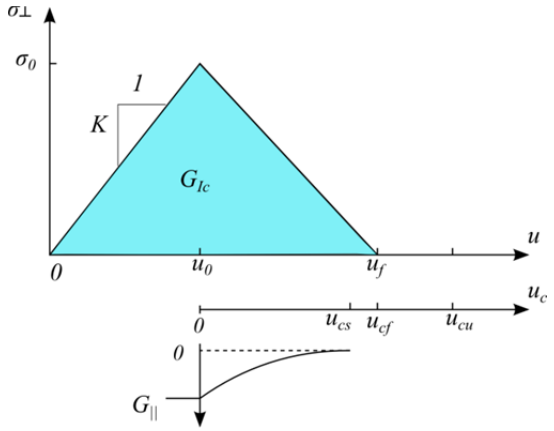

Fig. 5 Hillerborg model: tensile stress for Mode I cracking in function of relative nodal displacement and crack opening displacement; Shear stiffness reduction in function of crack opening displacement.

When a crack initiates, the fracture energy also consumes the elastic strain energy contained in the element up to that point. For the fracture energy to be consistent, the displacement at tensile failure should not be smaller than the displacement at crack initiation: $u_f \leq u_0$. This implies that there exists a maximum allowable element length $L_{e,max}$ for which the fracture energy can be represented correctly:

$$L_{e,\max} = \frac{2EG_{Ic}}{\sigma_0^2} \tag{4}$$

For a very brittle material such as glass, with a high stiffness and low fracture energy, this is quite a strict limit. Glass has an elastic modulus E = 70 GPa and fracture energy G_{Ic} = 7.8 J/m^2. With an estimated strength of 80 MPa, the critical element size would be $L_{e,max}$ = 0.17 mm. For the simulation of any realistically sized glass panel, the calculation times would become unfeasible when such a fine mesh should be used.

The unit element model of Fig. 2 is used to investigate how and whether the Hillerborg model in ABAQUS can be used when the critical element length is not respected. In addition to Table 2, the fracture energy G_{Ic} and crack opening displacements u_{cs} and u_{cu} need to be defined. The latter two are chosen sufficiently large: u_{cs} = 1.0 µm, and u_{cu} = 2.0 µm. The fracture energy is defined with respect to the element length L_e = 1 mm. The element length criterion, given by Eq. 4, is satisfied when $G_{Ic} \geq$ 50 J/m^2. The unit element model is evaluated for three cases: a) G_{Ic} = 100 J/m^2; b) 50 J/m^2; and c) 10 J/m^2. The evolution of the stresses in these simulations is given in Fig. 6.

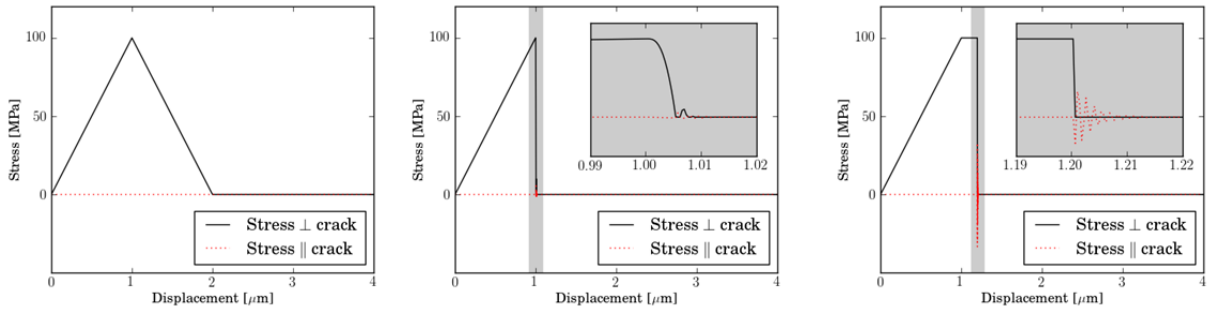

Fig. 6 Stress evolution for unit element model using Hillerborg failure model with a) G_{Ic} = 100 J/m^2, b) 50 J/m^2 and c) 10 J/m^2.

When the element length criterion is satisfied, the failure model behaves as expected from the above description. For a sufficiently high fracture energy, G_{Ic} = 100 J/m^2, a clear tensile softening behaviour is seen. The case where G_{Ic} = 50 J/m^2 should theoretically be equal to immediate failure upon reaching the criterion, as in the previous section. Nevertheless, a short softening phase over 10 time increments is seen, along with a small oscillation in the stress components due to the fast change in stiffness. But when the element length criterion is not satisfied, which would logically be the case when simulating a large glass component, a stress plateau is seen in Fig. 6c, rather than immediate failure. This pseudo-plastic behaviour continues until a work equivalent of twice the input fracture energy has been exerted after reaching the crack initiation criterion, as seen in Fig. 7. At that point, the tensile stiffness across the crack is reduced to zero within one time increment, which results in large oscillations in the stress components parallel to the crack face. As a consequence, some energy is dissipated by bulk viscosity already within the cracking element.

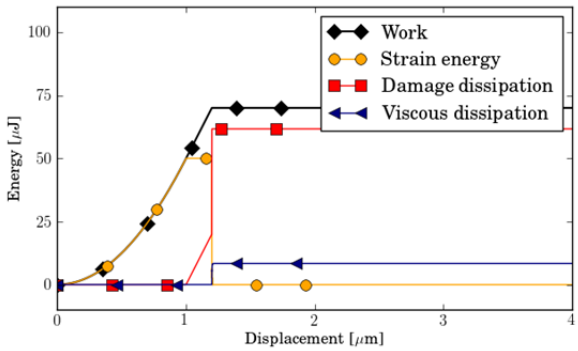

Fig. 7 Evolution of energies in function of displacement for unit element model using Hillerborg failure model with G_{Ic} = 10 J/m^2.

Thus, the material behaviour of the Hillerborg model, as implemented in ABAQUS, depends considerably on the element size. When the element length criterion is not satisfied, the dissipation by damage does not match the fracture energy, but overestimates it even more than when the input fracture energy would be artificially set to just satisfy the criterion. Moreover, an aggressive stiffness reduction causing stress oscillations within the element is seen.

3.3. Crack delay model for glass

Alternative formulations can be developed to bypass the issues that were identified previously. Moreover, a failure model may be designed to better capture the physical nature of glass fracture. Before discussing the implementation of a user-defined material model for ABAQUS/Explicit, the desired characteristics of an element deletion cracking model for glass are stipulated:

- Brittle fracture should occur fast, but a damage softening phase of finite duration should be present in order to avoid instabilities. The stiffness across the crack should be monotonously decreasing during this damage phase.
- Directionality of the crack should be taken into account to achieve realistic crack propagation.
- The element length criterion in Eq. 4 applies to any element deletion model. Thus, the fracture energy of glass will most likely be overestimated when using an element size that suits a practical engineering problem. However, this can be acceptable when the share of damage dissipation remains low compared to other energy quantities in the numerical analysis, e.g. post-fracture simulation of laminated glass.

- When a crack has initiated in an element, the subsequent constitutive behaviour should be independent of the element size as much as possible.

A possible cracking model that meets these requirements can be based on the concept of delay damage, as described for fibre reinforced plastics on the mesoscale by Allix et al. (2003). The main assumptions for such damage model are that (i) the evolution of damage due to variations of forces is not instantaneous, and (ii) a maximum damage rate exists, just as a maximum crack velocity exists. Another key issue is the identification of energy dissipated during fracture. The fracture surface energy G_{Ic} for a stationary crack in glass is a quite well-known value (see Table 1). This is defined as the energy required to separate two newly created free surfaces and can be associated with a characteristic length u_{cf} in a cohesive traction-separation law:

$$G_{Ic} = \int_0^{u_{cf}} \sigma_{\perp} du_c \,, \tag{5}$$

where u_c is the crack opening width. At $u_c = u_{cf}$, the crack surfaces are fully separated and the traction $\sigma_{\perp}$ should be nullified. The traction-separation law can be described by a single scalar damage parameter d, defined as the relative variation of the elastic modulus:

$$\sigma_{\perp} = E_0(1-d)\langle\varepsilon\rangle \; - E_0\langle-\varepsilon\rangle \;, \tag{6}$$

where $\langle\cdot\rangle$ denote Macaulay brackets, used to distinguish the behaviour in tension and in compression, and E_0 is the Young's modulus for undamaged material.

The damage function $d(u_c)$ for quasi-static behaviour should be monotonically increasing with the crack opening width, such that:

$$\begin{cases} d(u_c \le 0) = 0 \\ d(u_c \ge u_{cf}) = 1 \end{cases} \tag{7}$$

Moreover, the damage is irreversible, i.e. the damage parameter d cannot decrease when the crack opening width decreases. Assuming linear behavior of the traction-separation relation, the damage increment can be written as:

$$\Delta d = \max\left(\Delta\varepsilon_{\perp} / \varepsilon_{cf}, 0\right), \tag{8}$$

where $\Delta\varepsilon$ is the incremental strain in the direction perpendicular to the crack and $\varepsilon_{cf} = u_{cf}/L_e$ with L_e being the characteristic size for the considered element. The crack opening width at failure u_{cf} can in turn be calculated as:

$$u_{cf} = 2G_{Ic} / \sigma_0 \,, \tag{9}$$

where σ_0 is the fracture strength of the material for a brittle failure mode defined by the Rankine criterion.

Under dynamic loading, the damage increment should be bounded by a maximum damage rate $\dot{d}_{max}$:

$$\Delta d \le \dot{d}_{\max} \Delta t \tag{10}$$

This maximum damage rate can be linked to the maximum crack velocity v_c which is a physical property for brittle materials. Suppose that a crack initiates at one edge of the element. Then the crack tip may not cross the element by a speed greater than v_c. Or otherwise stated, the damage may not increase at a rate faster than the crack can run through the element, i.e.:

$$\dot{d}_{\max} = v_c / L_e \tag{10}$$

The described material behaviour is schematically represented in Fig. 8. The required input parameters to define the cracking behaviour for this material model are (i) the strength σ_0, (ii) the fracture energy G_{Ic} for a stationary crack, and (iii) the maximum crack velocity v_c. These are all physical material properties that are valid regardless of the

element size. Also, the stress calculation in the damage phase takes account of the direction of the crack by rotation of the local coordinates system to the eigenvectors at the moment of crack initiation.

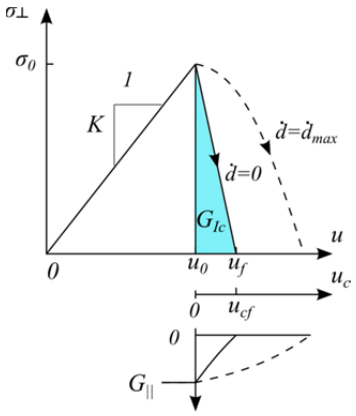

Fig. 8 Crack delay model: tensile stress for Mode I cracking in function of relative nodal displacement and crack opening displacement; Shear stiffness reduction in function of crack opening displacement.

A few notes can be made regarding the physical interpretation of this failure model:

- The fracture energy G_{Ic} used as input parameter is defined as the energy needed to create two free surfaces by cracking. In the material model, an opening crack is not modelled explicitly (because this would require element enrichment such as in XFEM), but rather its effect on the element stiffness is taken into account. In the simulation output, damage dissipation is defined as the difference between the work performed on the element and the strain energy. For the quasi-static case, this means that the dissipated energy by fracture of an element amounts to G_{Ic} added with the strain energy that is present in the element prior to cracking.
- In the dynamic case, the damage rate is bounded by the crack propagation velocity. Then it is possible that $\Delta d < \Delta\varepsilon / \varepsilon_{cf}$. Consequently, the effective fracture energy can also be greater than G_{Ic}. However, as shown by Sharon and Fineberg (1999), the experimentally measured fracture energy of a crack propagating at v_c also appears greater than the fracture energy for a stationary crack.
- The maximum crack propagation velocity cannot be enforced on the global scale. It is possible that damage increases for several adjacent elements simultaneously, such that the propagation velocity of the simulated crack appears greater than v_c. This will not likely be the case for a realistic engineering problem, but it is not prohibited by the current material formulation either.

The crack delay model is evaluated for the unit element model of Fig. 2. In addition to the material properties given in Table 2, the fracture energy for a stationary crack G_{Ic} and the maximum crack propagation speed v_c need to be defined. In this example, $G_{Ic} = 10\,\text{J/m}^2$. The choice of the crack velocity is based on the ratio of the crack velocity to the dilatational wave speed for glass, i.e. 1500 / 5697 = 0.26. For the unit element, the dilatational wave speed is c_d = 6.93 m/s; then v_c/c_d = 0.28 when v_c = 2.0 m/s. However, the unit element is slowly strained by predefined displacement of its nodes. This implies that the damage rate will not be surpassed in this example, unless a much smaller v_c is used. Hence the second value v_c = 0.01 m/s for which the material model is evaluated. Fig. 9 shows the evolution of the stress orthogonal to the developing crack (a), as well as the energies (b). The stress components parallel to the crack faces are zero for this quasi-static case.

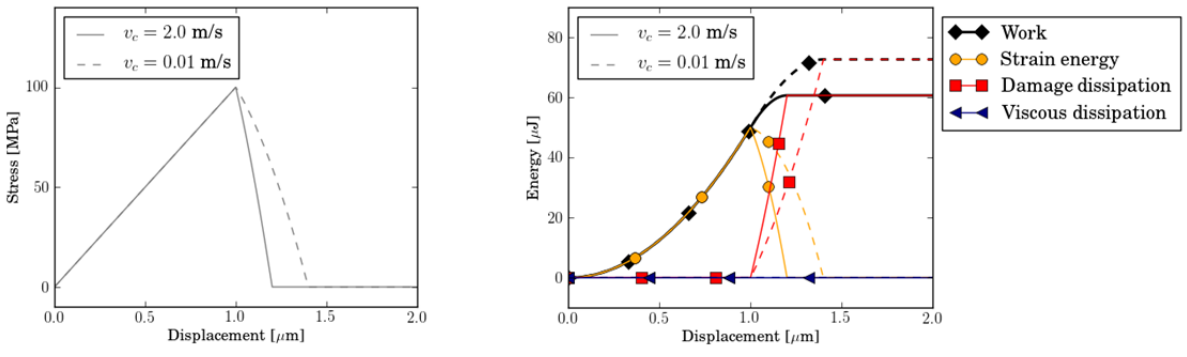

a) b)

Fig. 9a) Stress perpendicular to crack face, and b) Energies in function of displacement for unit element with crack delay model.

This figure demonstrates the delay effect for the damage evolution. For v_c = 2.0 m/s, the material model behaves as defined for the static case, where the stress is reduced to zero at the predefined cracking strain. When v_c = 0.01 m/s, the damage is delayed and the stress in the element only becomes zero at a higher strain. This is reflected in the energy balance, where the dissipated energy is larger when the delay effect is active.

The influence of the damage delay becomes clearer when the failing element is surrounded by other elements whose elastic springback in response to the damage poses a dynamic load. Therefore, the controlled problem with three unit elements introduced in Section 3.1 is revisited. An assessment is made for several settings of the crack velocity around 2.0 m/s, and for the case where the fracture energy is set to a small value. A special case is found when the crack velocity is set greater than the ratio of the element size L_e to the stable time increment Δt. Then, the damage rate in the model can never reach the limiting damage rate as defined by Eq. 10. With a stable time increment $\Delta t = 1.243 \cdot 10^{-4}$ s, the ratio $L_e/\Delta t$ = 8.05 m/s.

The stress decay in the damage phase is given in Fig. 10 for different settings of v_c and G_{Ic}. For all given cases, the stiffness is reduced to zero quickly over a few time increments. The delay of the damage evolution becomes active when v_c < Le/Δt, in which case the stress decay takes place less abruptly with smaller values for $\dot{d}_{max}$. Smaller fracture energy, on the other hand, implies a steeper gradient in the traction-separation law schematically given by Fig. 8, and thus more aggressive fracture behaviour.

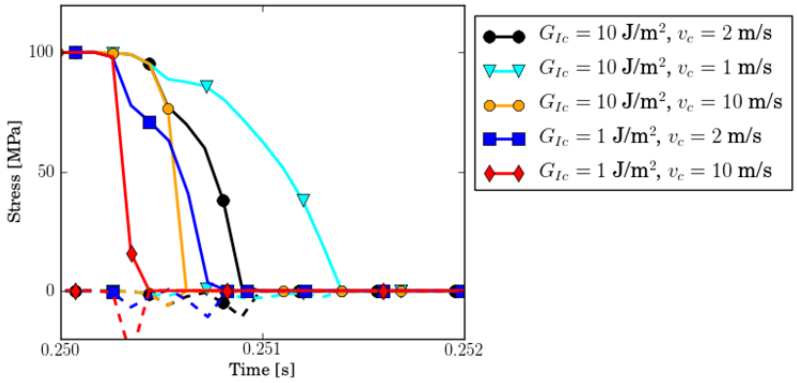

Fig. 10 Stress decay of failing element for model with three unit elements using a crack delay model; solid and dashed lines for stress components orthogonal and parallel to the crack face respectively.

The energy evolution in these simulations is similar to that of Fig. 4. The work, damage and viscous dissipations at the end of the simulations are given in Table 3 for the different settings of v_c and G_{Ic}. For all cases, the strain energy is zero at the end of the simulation.

These results show that the delay effect aids in reducing stress oscillations upon failure of an element. However, this comes with a higher damage dissipation, which can be interpreted as an overestimation of the effective fracture energy. The effectiveness and validity of the crack delay model should be further investigated for realistic cases of glass fracture. That is the aim of the following sections.

Table 3: Work and dissipations at end of simulation for three unit elements model with crack delay.

Material properties	Work	Damage dissipation	Viscous dissipation
G_{Ic} = 10 J/m^2, v_c = 1.0 m/s	151.2 µJ	134.0 µJ	17.2 µJ
G_{Ic} = 10 J/m^2, v_c = 2.0 m/s	150.8 µJ	112.9 µJ	37.9 µJ
G_{Ic} = 10 J/m^2, v_c = 10.0 m/s	150.6 µJ	62.3 µJ	88.3 µJ
G_{Ic} = 1 J/m^2, v_c = 2.0 m/s	150.6 µJ	114.1 µJ	36.5 µJ
G_{Ic} = 1 J/m^2, v_c = 10.0 m/s	150.3 µJ	54.8 µJ	95.5 µJ

4. Drop weight impact on monolithic glass

The drop weight experiments used for comparison of simulations in this section are performed on a well-instrumented, in-house test setup (Van Dam et al. 2014). This test setup consists of a steel impactor mounted on guiding rails with low friction, and a rigid support base in which a test specimen is held between polypropylene rings. The considered tests were performed on circular glass plates with a diameter of 100 mm and thickness of 4.0 mm (as measured). Compressive clamping conditions exist by tightening of bolts on steel clamping rings with a total force of 5.5 kN. The impactor is fitted with a rigid steel tip of 10 mm in diameter and has a total mass of 7.38 kg. The drop height in the experiments is 200 mm, for which the impactor hits the glass at a speed of 1.980 m/s.

The simulation of this experiment has been investigated earlier in (Pelfrene et al. 2013). In this article, it was concluded that it is necessary to model the boundary conditions realistically; with the polypropylene rings as deformable parts. The impactor may be modelled as a rigid tip with inertia assigned to it. Compressive clamping conditions should be taken into account for motions in the post-fractured state. It was also seen that the glass part meshed by hexahedral elements suffers from an unphysical delay in fragmentation, because the last element through the thickness at a crack location is not able to capture the bending stresses correctly. A finer mesh with tetrahedral elements experiences this problem far less and better allows the modelling of fragmentation of the glass specimen. In (Pelfrene et al. 2016), it was seen that an unstructured mesh with more uniform element sizes favours the more natural finding of a realistic cracking pattern. A similar conclusion has been drawn by Song et al. (2006).

An axisymmetric representation of the numerical model is given in Fig. 11. The stresses in axial direction due to compressive clamping conditions are included in this figure for the glass and polypropylene parts. The stress and deformation field is calculated for static loading with the implicit solver in ABAQUS and is subsequently imported for impact analysis with the explicit solver. Material parameters for soda-lime silicate glass and polypropylene are given in Table 4.

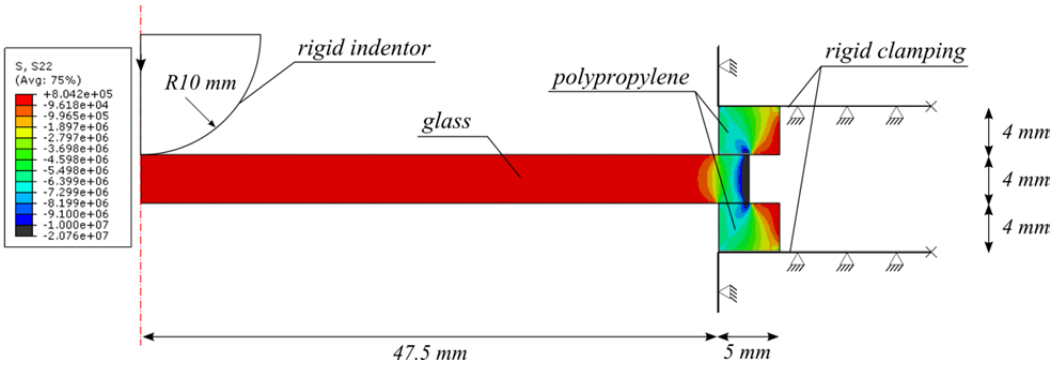

Fig. 11 Axisymmetric representation of numerical model for drop weight impact on glass specimen with boundary conditions and compressive clamping; contours of initial stress field in axial direction.

Table 4: Material properties for drop weight impact simulation

		Soda-lime silicate glass	Polypropylene
Young's modulus	E	70 GPa	1.3 GPa
Poisson's ratio	ν	0.23	0.42
Fracture strength	σ_0	255 MPa	
Density	ρ	$2.5 \cdot 10^3$ kg/m^3	900 kg/m^3

The glass strength is the most distinctive parameter for the cracking behaviour in the numerical simulation. However, to pin down a value for the strength is not self-evident because of the very high variability that is observed experimentally. The critical stress in Table 4 is motivated by the average strength measured in quasi-static testing, increased by influence of the loading rate. De Pauw (2009) performed ball-on-ring tests for axisymmetric bending up to failure. The test specimens were of the same size and shape, and of the same production batch as those used in the drop weight impact. The flexural strength in these tests was on average 150 MPa. The loading rate in the impact tests at a drop height of 0.2 m is about $3.5 \cdot 10^5$ MPa/s. With the curve in Fig. 1, a strength that is 70% higher than the quasi-static value may be expected at this loading rate.

The three failure models discussed in the previous section are evaluated for their ability to capture the dynamic cracking and fragmentation of the monolithic glass sample in the drop weight impact test.

4.1. Immediate element failure

The immediate failure model is assigned to the glass elements for a mesh that consists of 222,000 elements with average element length L_e = 1.0 mm. The deceleration of the impactor is given in Fig. 12 in comparison with a representative experimental measurement. From the figure, it seems that the resistance of the glass to the impactor quickly vanishes and compares quite well with the experiment. However, the cracks and fragmentation in Fig. 13 show that the technique of immediate element removal does not at all reproduce a realistic cracking behaviour. This most likely stems from the absence of a damage phase in which the crack direction is taken into account for softening of the elastic stiffness.

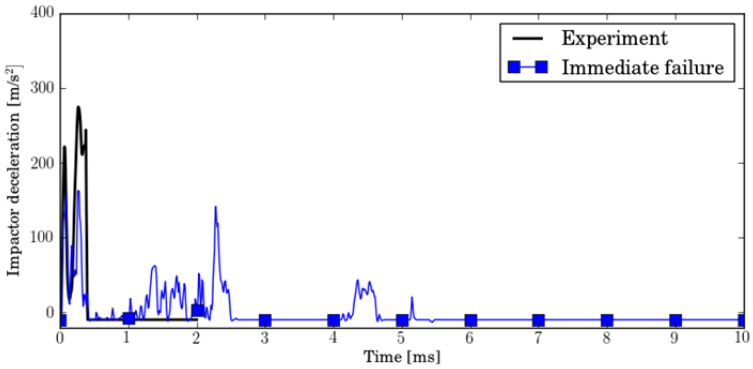

Fig. 12 Comparison of simulation results of glass with immediate failure model to experimental data for drop weight impact.

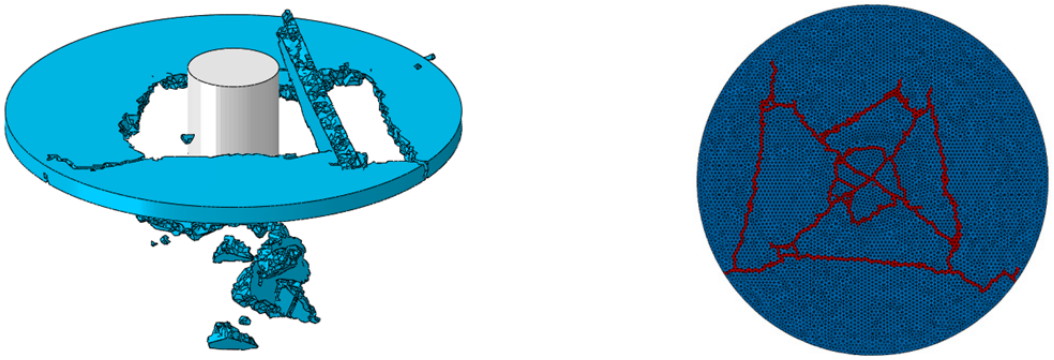

a) b)

Fig. 13 Glass cracking and fragmentation at t = 10ms for drop weight impact simulation with immediate failure model; a) perspective view, b) bottom view of failed elements.

4.2. Hillerborg model

For the simulation of glass fracture with the Hillerborg model in ABAQUS, a few additional material parameters need to be defined. With reference to Table 1, the fracture energy for soda-lime silicate glass is set as G_{Ic} = 7.8 J/m^2. For this fracture energy, the element length criterion is not satisfied for any element in the mesh. The crack opening displacements for shear failure u_{cs} and ultimate failure u_{cu} can be chosen the same as the crack displacement for tensile failure u_{cf}. When the element length criterion is not satisfied, u_{cf} is given by Eq. 9 for the Hillerborg model as well. Consequently, $u_{cf} = u_{cs} = u_{cu} = 6.12 \cdot 10^{-8}$ m.

Fig. 12 shows the fragmentation of the glass part at the end of the simulation. The first radial cracks are formed at t = 0.3 ms in the simulation, which corresponds well with the experiment. It takes more time before the next fragments are formed by further, concentric, cracking which happens quickly around t = 2.0 ms. While in the experiment about 40 radial and 20 concentric cracks appear, much less are formed in the simulation. It could be expected that a finer mesh allows for more cracks to be formed. Therefore, the analysis is repeated for a refined mesh. A mesh with average element length $L_{e,avg}$ = 0.75 mm, however, already consists of more than 500,000 elements. With this refinement, no major differences are noted in the global behaviour of the model. This is confirmed by the evolution curves for the impactor deceleration, given in Fig. 13. It is clear from this figure that the impactor is decelerated much more in the simulation than it is in reality. A faster fragmentation cannot be forced on the numerical analysis.

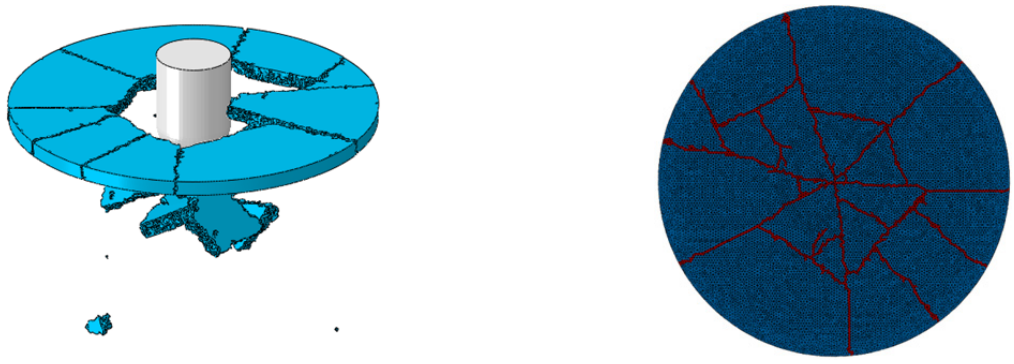

a) b)

Fig. 12 Glass cracking and fragmentation at t = 10ms for drop weight impact simulation with immediate failure model; a) perspective view, b) bottom view of failed elements.

The evolution of the energies in the simulation is given in Fig. 14. The kinetic energy lowers considerably in the first stage of the impact, corresponding with the deceleration of the impactor. The amount of viscous dissipation is due the damping of stress waves in the material that originate from the fast stress release in the cracked elements. The frictional dissipation results primarily from the glass fragments vibrating while being held between polypropylene clamping rings. It would be expected that the elastic strain energy in the model goes back to zero when all cracks have been formed and the impactor experiences no further resistance of the glass. Instead it is seen that the strain energy remains rather high, while the damage dissipation is almost negligible. On closer inspection, it is seen that the failed and deleted elements in the model have a constant, non-zero, and indeed quite high strain energy assigned to them after they have failed. In that situation these elements are unable to carry stresses, which means that this remaining strain energy is not physical. This seems to be a bug in the built-in material model and it would be more logical to interpret this part of the strain energy as damage dissipation.

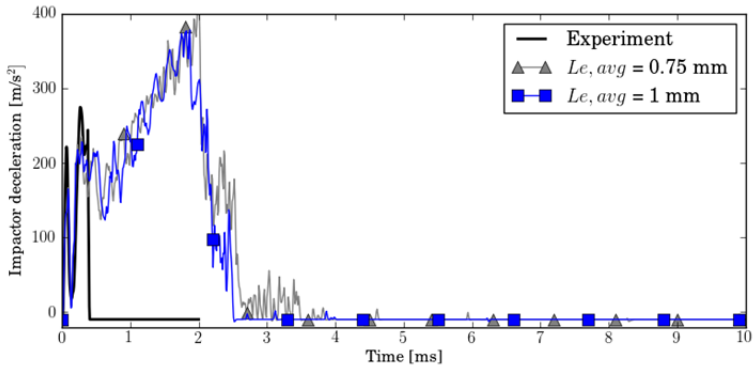

Fig. 13 Comparison of simulation results of glass with immediate failure model to experimental data for drop weight impact.

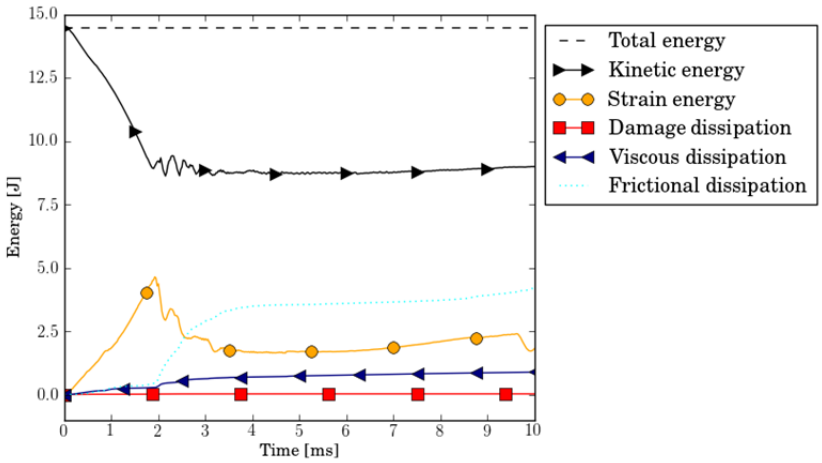

Fig. 14 Evolution of energies in simulation of glass with Hillerborg material model under drop weight impact.

4.3. Crack delay model

The cracking behaviour of the crack delay model is governed by σ_0, v_c and G_{Ic}. The fracture energy of a stationary crack and the maximum crack velocity are physical constants for soda-lime glass and amount to G_{Ic} = 7.8 J/m^2 (see Table 1) and v_c =1500 m/s. The latter is less than three times smaller than the dilatational wave speed in glass (c_d = 5697 m/s). Taking account of the CFL condition used to calculate the stable time increment, it can be noted that a minimum of 4 Δt are needed for the stress decay of the smallest element when the damage rate is limited. A slightly longer duration is needed for larger elements in failure. Thus, also for this failure model, it is recommended to mesh the glass with a more uniform element size.

Fig. 15 shows the simulated cracks and fragmentation that follow from the crack delay model. Great similarity with the built-in Hillerborg model is seen, both in the number of cracks and the size of the fragments. For this reason, the deceleration of the impactor in the simulation is given in comparison with the result from the analysis using the Hillerborg model in Fig. 16. This figure shows that cracking and full fragmentation of the simulated specimen occurs quicker with the crack delay model and that the impactor is slowed down less than for the Hillerborg model. This is an improvement, although the crack formation is still not as quick as in the experiment.

The energies are given in Fig. 17. In comparison with the Hillerborg model (see Fig. 14), the impactor keeps more of its kinetic energy, which is consistent with the trend of the deceleration. The viscous dissipation is smaller, which indicates that the damage delay effectively reduces stress oscillations. The elastic strain energy does return to zero after all cracks have formed.

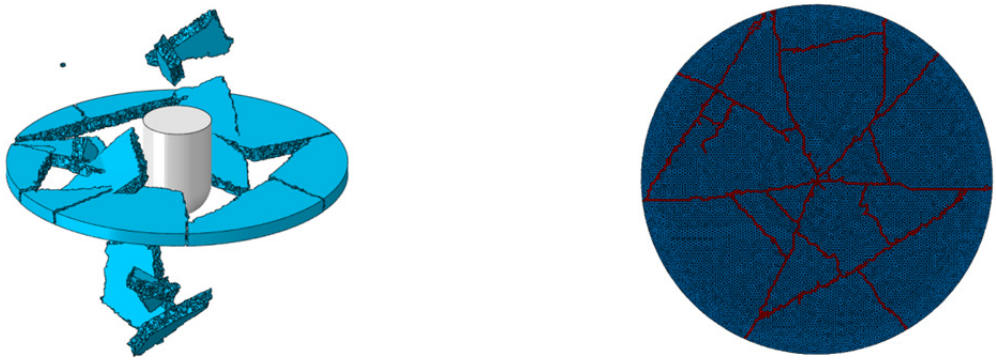

a) b)

Fig. 16 Glass cracking and fragmentation at t = 10ms for drop weight impact simulation with immediate failure model; a) perspective view, b) bottom view of failed elements.

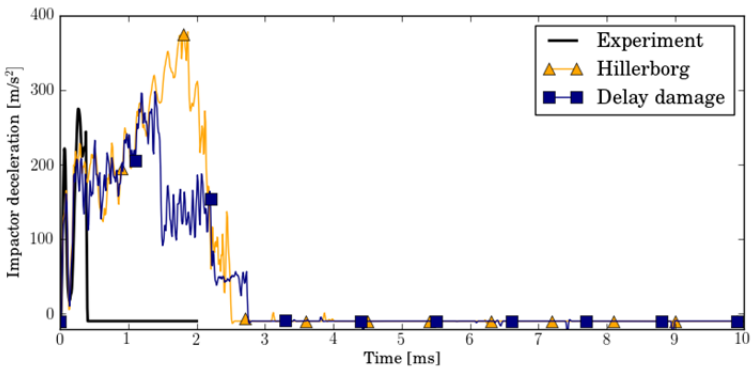

Fig. 15 Comparison of simulation results of glass with immediate failure model to experimental data for drop weight impact.

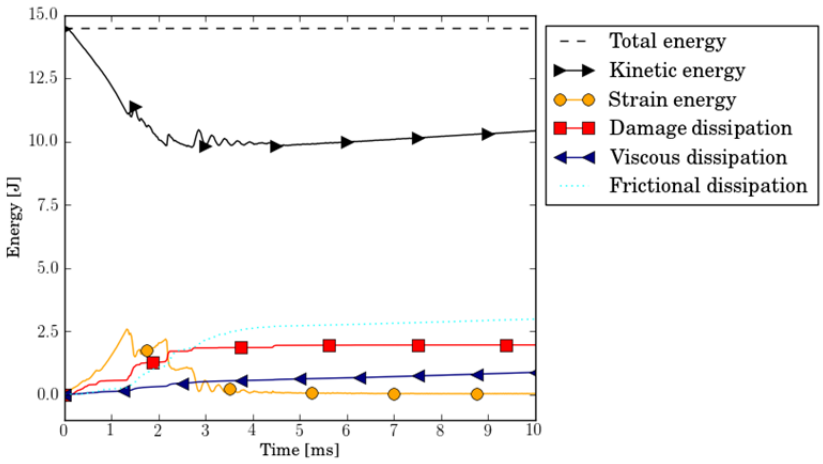

Fig. 16 Evolution of energies in simulation of glass with crack delay failure model under drop weight impact.

In conclusion, the crack delay model is a more theoretically correct implementation for glass cracking by element deletion. Moreover, its behaviour is designed to be independent of the element length, although it is still recommended to use a more uniform element size. It is seen that the damage delay becomes active under dynamic loads and, as a side effect, lowers the stress oscillations in the surrounding elements which is beneficial for the stability of the simulation. In an impact simulation, a credible fragmentation can be simulated which is in part achieved by taking account of the crack directionality.

5. Conclusions

Three failure models for element deletion have been characterized using a simple unit element model and have further been evaluated for their ability to capture the cracking and fragmentation of a monolithic glass plate under drop weight impact. Several issues can be identified:

- When stiffness is reduced in an element, the loss in strain energy is regarded as dissipation by damage. This energy surpasses the physical fracture energy if the element size is greater than a critical length.
- If no damage phase is present in the failure model or the damage rate is not limited, the immediate erosion of stiffness in an element can cause stress waves of high amplitude in the surrounding elements. This may lead to spurious failure in other zones of the mesh by wave reflection.
- If the directionality of the crack in an element is not taken into account, radial and concentric cracks in glass are not reproduced with a correct pattern and formation sequence.

It is also seen that when the element length criterion for the fracture energy is not satisfied, the Hillerborg model as implemented in ABAQUS behaves differently; with a pseudo-plastic phase instead of damage softening. Also, a bug in the implementation seems to exist for the calculation of post-cracked strain energy and damage dissipation.

For these reasons a failure model is proposed to better capture the physical nature of glass cracking and to avoid numerical instabilities. Still, also with this model it is seen that fewer glass cracks appear in the simulation than in reality, and that they appear slower, thus reducing the kinetic energy. It can be expected that substantial mesh refinement would improve both aspects, but the mesh for the monolithic glass sample already consists of a high number of elements. However, this may not be an issue for the simulation of a realistically sized laminated glass panel. In that case, the mesh can be constructed with shell elements and the impact duration is typically higher as well.

In general, the element deletion technique is highly mesh-dependent for local cracking behaviour, but it can be seen that global results for different meshes do agree. For practical engineering problems it is often sufficient to have knowledge of the global quantities, such as the forces that act on the surrounding structure during the impact and energy absorption by material failure. The crack delay model offers an improved manner to achieve this for cracking of structural glass components.

References

Allix, O., Feissel, P., Thevenet, P.: A delay damage mesomodel of laminates under dynamic loading: basic aspects and identification issues. Comp. Struct. 81, 1177-1191 (2003)

Beason, W.L., Morgan, J.R.: Glass failure prediction model. J. Struct. Engng. 110(2), 197-212 (1984)

Behr, R., Karson, M., Minor, J.: Reliability analysis of window glass failure pressure data. Struct. Safety 11, 43-58 (1991)

Belytschko, T., Lu, Y.Y., Gu, L.: Crack propagation by element-free Galerkin methods. Engng. Fract. Mech. 51, 295-315 (1995)

Brajer, X., Hild, F., Roux, S.: On the dynamic fragmentation of glass: a meso-model. Int. J. Fract.163, 121-131 (2010)

Camacho, G.T., Ortiz, M.: Computational modeling of impact damage in brittle materials. Int. J. Solids Struct. 33(20-22), 2899-2983 (1996)

DIN EN 13541:2012. Glass in building – security glazing – Testing and classification of resistance against explosion pressure (2012)

Clif, C.J.: Fracture of glass under various liquids and gases. J. Soc. Glass Tech. 41, 157-167 (1957)

De Pauw, S.: Experimental and numerical study of impact on window glass fitted with safety window film. Doctoral dissertation, Ghent University (2010)

Gehrke, E., Ullner, C., Hähnert, M.: Correlation between multistage crack growth and time-dependent strength in commercial silicate glasses, Part 1: Influence of ambient media and types of initial cracks. Glastechnisches Bericht 60(8), 268-278 (1987)

Griffith, A.A.: The phenomena of rupture and flow in solids. Phil. Trans. R. Soc. Lond. B 221, 163-198 (1921)

Hillerborg, A., Modeer, M., Peterson, P.-E.: Analysis of crack formation and crack growth in concrete by means of fracture mechanics and finite elements. Cem. Concr. Res. 6, 773-782 (1976)

Irwin, G.R.: Analysis of stresses and strains near the end of a crack traversing a plate. J. Appl. Mech. 24, 361-364 (1957)

Johnson, G.R., Stryk, R.A., Beissel, S.R., Holmquist, T.J.: An algorithm to automatically convert distorted finite elements into meshless particles during dynamic deformation. Int. J. Imp. Engng. 27, 997-1013 (2002)

Kuntsche, J., Schneider, J.: Mechanical behavior of polymer interlayers in explosion resistant glazing. In: Louter, C., Belis, J., Bos, F., Lebet, J., editors. Challenging Glass 4 and COST Action TU0905 Final Conference. United Kingdom: Taylor Francis ltd., pp. 447-454 (2014)

Linger, K.R., Holloway, D.G.: The fracture energy of glass. Phil. Mag. 18(156), 1269-1280 (1968)

Louter, C., Nielsen, J.H.: Numerical analyses of the effect of SG-interlayer shear stiffness on the structural performance of reinforced glass beams. In: Louter, C., Mocibob, D., editors. COST Action TU0905 Mid-Term Conference. United Kingdom: Taylor Francis ltd., pp. 405-412 (2013)

Moës, N., Dolbow, J., Belytschko, T.: A finite element method for crack growth without remeshing. Int. J. Num. Meth. Engng. 46, 131-150 (1999)

Nie, X., Chen, W.W., Templeton, D.W.: Dynamic ring-on-ring equibiaxial flexural strength of borosilicate glass. Int. J. Appl. Ceram. Tech. 7(5), 616-624 (2010)

Pelfrene, J., Kuntsche, J., Van Dam, S., Van Paepegem, W., Schneider, J.: Critical assessment of the post-breakage performance of blast loaded laminated glazing: experiments and simulations. Int. J. Imp. Engng. 88, 61-71 (2016)

Pelfrene, J., Van Dam, S., Van Paepegem, W., Degrieck, J.: Numerical simulation of elastic, fracture and post-failure response of monolithic and laminated glass under impact loading. In: Louter, C., Mocibob, D., editors. COST Action TU0905 Mid-Term Conference. United Kingdom: Taylor Francis ltd., pp. 413-420 (2013)

Peng, Y., Yang, J., Deck, C., Willinger, R.: Finite element modelling of crash test behaviour for windshield laminated glass. Int. J. Imp. Engng. 57, 27-35 (2013)

Sharon, E., Fineberg, J.: Confirming the continuum theory of dynamic brittle fracture for fast cracks. Nature 397, 333-335 (1999)

Song, J.H., Wang, H., Belytschko, T.: Comparative study on finite element methods for dynamic fracture. Comp. Mech. 42, 239-250 (2006)

Surdyka, N.D., Pantano, C.G., Kim, S.H.: Environmental effects on initiation and propagation of surface defects on silicate glasses: scratch and fracture toughness study. Appl. Phys. A 116, 519-528 (2014)

Van Dam, S., Pelfrene, J., De Pauw, S., Van Paepegem, W.: Experimental study on the dynamic behaviour of glass fitted with safety window film with a small-scale drop weight set-up. Int. J. Imp. Engng. 73, 101-111 (2014)

Veer, J., Rodichev, Y.: The structural strength of glass: hidden damage. Strength Mat. 43, 302-315 (2011)

Wiederhorn, S.M.: Fracture surface energy of glass. J. Am. Ceram. Soc. 52(9), 99-105 (1969)